Tectonophysics 686 (2016) 19–26

Contents lists available at ScienceDirect

Tectonophysics

journal homepage: www.elsevier.com/locate/tecto

Flexure and gravity anomalies of the oceanic lithosphere beneath the Louisville seamount

Gyuha Hwang [a], Seung-Sep Kim [a,b,*]

[a] Geology and Earth Environmental Sciences, Chungnam National University, 99 Daehak-ro, Yuseong-gu, Daejeon, 34134, Republic of Korea
[b] Department of Astronomy, Space Science and Geology, Chungnam National University, 99 Daehak-ro, Yuseong-gu, Daejeon 34134, Republic of Korea

ARTICLE INFO

Article history:
Received 5 April 2016
Received in revised form 14 July 2016
Accepted 18 July 2016
Available online 20 July 2016

Keywords:
Lithospheric flexure
Dense core seamount
Louisville Seamount Chain

ABSTRACT

We have calculated the elastic thickness (T_e), flexural deflection, and gravity anomaly of the oceanic crust beneath the Louisville seamount (LSC-03), near the Kermadec trench. A regional-residual separation of the bathymetry was performed to remove the effect of other geologic features (e.g., the trench). We used the uniform density and dense core models to approximate the total mass of the seamount, which was defined as the surface load required for flexural deformation. From the flexure modeling results, we found that more flexural depression was predicted by the uniform density model than by the dense core model. However, the uniform density model predicted a significantly smaller gravity anomaly than observed, whereas the dense core model minimized the prediction misfits reasonably. The best flexure model was found with a T_e of 16 km for the uniform density model and 6 km for the dense core model. The flexure computed with the dense core model was consistent with the seismically detected Moho. The flexure modeling for LSC-03, thus, indicates that the dense core model better approximates the inner structure of the LSC-03. Based on the crustal age and geochronology of the given seamount, the age of the oceanic crust at the time of seamount formation (Δt) is 20 Ma. If this is the case, however, the T_e estimates from both flexure models require some degree of lithospheric reheating by Louisville hotspot activity. Alternatively, considering the tectonic plate motion of the Osbourn Trough, Δt becomes approximately 4 Ma. This younger lithosphere model is more consistent with the observed flexural deformation and the T_e estimate from the dense core model. Therefore, the time that the seamount-induced lithospheric deformation occurred may be far earlier than the age-dated volcanism.

1. Introduction

Lithospheric flexure describes deformation resulting from a geological load (e.g., seamounts and oceanic islands) above the elastic oceanic plate. The lithospheric flexure is therefore determined by the balance between the finite strength of the elastic plate, the driving force, and the restoring force (i.e., buoyancy of the mantle) (Watts, 2001). Because elastic plate strength depends on its effective thickness (T_e), the lithospheric flexure is simply expressed in terms of T_e when the shape (e.g., bathymetry) and mass of the seamount are known. In general, the thicker the T_e of the oceanic crust, the higher the flexural rigidity for resisting a given load, and the smaller the flexure. To investigate the causal relationship between lithospheric deformation and underwater volcanism, many researchers have estimated T_e beneath seamounts and ocean islands at various locations (e.g., Adam and Bonneville, 2008; Calmant, 1987; Collier and Watts, 2001; Hu et al., 2015; Kim and Wessel, 2010; Watts et al., 2006; Wessel, 1993).

In flexure modeling constrained by gravity anomalies, there are trade-offs between positive anomalies generated by the volcanic construct (e.g., seamount) and negative anomalies due to lithospheric deformation (i.e., flexure). Minimizing the misfits between the observed and predicted gravity anomalies, however, cannot resolve such inherent trade-offs related to the actual geologic structures. For example, more flexure can be estimated to minimize the gravity misfits, although the misfits can also be reduced by changing the density model of the given seamount (e.g., Kim and Wessel, 2010; Minshull and Charvis, 2001).

The uniform density model is the most commonly used density model for seamounts (e.g., Calmant et al., 1990; Hillier, 2007; Hu et al., 2015). This model greatly reduces computational efforts required for calculating gravity anomalies because the boundaries between bodies of different densities can be simplified. However, the uniform density model has a tendency to bias T_e estimates because of its simplified density structure (e.g., Kim and Wessel, 2010; Minshull and Charvis, 2001). In particular, Kim and Wessel (2010) pointed out that the uniform density model tends to overestimate the total mass of the seamount and hence increase T_e to account for the extra mass. As an alternative density model, they proposed the dense core model that divides a seamount into dense core, edifice, and sedimentary peripheral layers, in order to approximate the observed inner structure of seamounts (e.g., Araña et al.,

* Corresponding author at: Geology and Earth Environmental Sciences, Chungnam National University, 99 Daehak-ro, Yuseong-gu, Daejeon, 34134, Republic of Korea.
E-mail address: seungsep@cnu.ac.kr (S.-S. Kim).

http://dx.doi.org/10.1016/j.tecto.2016.07.014
0040-1951/

2000; Camacho et al., 2009; Contreras-Reyes et al., 2010; Gallart et al., 1999; Hammer et al., 1991). Therefore, in this study, we aim to estimate the lithospheric strength under the Louisville seamount using the dense core model.

The Louisville Seamount Chain (LSC) is located on the Pacific Plate, and is currently being subducted beneath the Indo-Australian plate at the Tonga-Kermadec Trench (Fig. 1). For this study, we investigate the flexural deformation beneath the LSC-03 seamount, the third LSC seamount from the subduction zone (see red circle in Fig. 1). The $^{40}Ar/^{39}Ar$ age of LSC-03 is 69.65 ± 0.48 Ma (Koppers et al., 2004, 2011) and the age of the oceanic crust is 89.65 ± 1.52 Ma (Müller et al., 2008). In order to examine the relative contribution of magma to lithospheric flexure of the LSC-03, Contreras-Reyes et al. (2010) conducted a wide-angle seismic refraction survey (profile A-B in Fig. 1). Their seismic study revealed the seismically constrained flexed Moho and the dense core located 1.5 km below the edifice of the LSC-03. Thus, the LSC-03 is an optimal candidate for examining the effects of a chosen density model on flexure estimation. We employ both the dense core and uniform density models and compare the predicted results with the observed gravity and seismic Moho. Using the T_e estimates, we also discuss the timing of the LSC-03 formation.

2. Methods

High-resolution bathymetry is a crucial tool for defining the shape of seamounts. However, the bathymetric data also contain regional geologic structures (e.g., trench and swell), unrelated to the seamounts of interest. In order to separate the LSC-03 from the regional bathymetry, we performed regional-residual separation of bathymetry data using spatial filters (Kim and Wessel, 2008; Wessel, 1998, 2016). For this study, we utilized the SRTM30_PLUS v11 (Becker et al., 2009), which incorporated calibrated shipboard bathymetry with satellite-derived depths (Fig. 1).

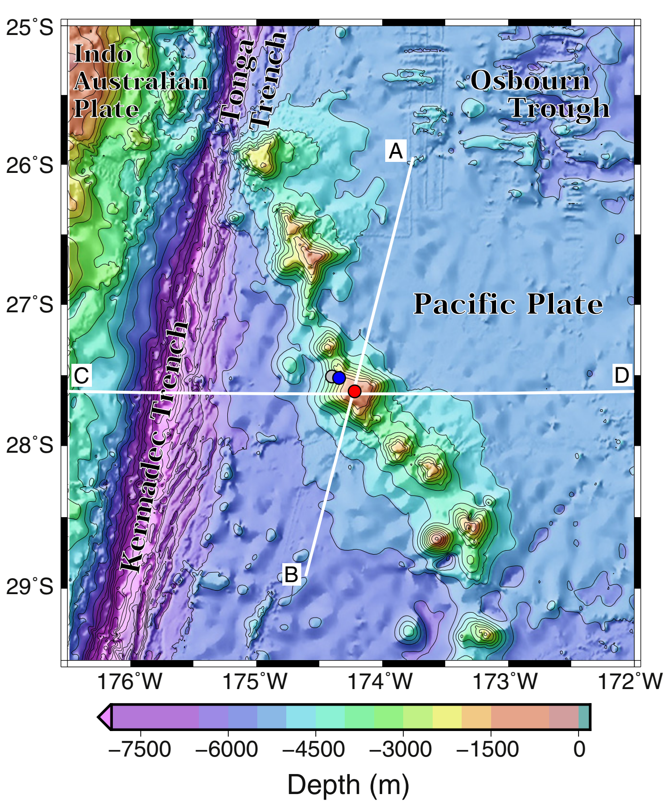

Fig. 1. Bathymetry of the northern Louisville Seamount Chain (LSC). The background data is SRTM30_PLUS v.11.0 (Becker et al., 2009). Some important tectonic structures are shown. The red circle is the location of seamount LSC-03, the gray and blue circles are the sampling locations from Koppers et al. (2004) and Koppers et al. (2011), respectively, and profile A-B is the seismic line of Contreras-Reyes et al. (2010). Contour interval is 500 m.

Two types of spatial filters were used to capture the regional bathymetry, in particular, the rapid variations in depth near the Kermadec-Tonga Trench: traditional median and directional median (DiM) filters. The DiM filter is a modified version of the median filter, which divides a given filter circle into N "bow-tie" sectors to determine the lowest median value from N median values of the sectors (Kim and Wessel, 2008). It can be effective in circumventing biased estimates of regional trends because the traditional median filter is not able to accurately separate small structures from the inclined plane (Wessel, 1998).

In addition, the separation result is sensitive to the choice of filter width. In order to define an optimal filter width for effective separation, the optimal robust separation (ORS) method was utilized (Wessel, 1998). The ORS method computes mean amplitudes (i.e., the ratio of volume to area of the residual bathymetry), which tend to be maximized when the separation is optimized. The residual bathymetry is simply obtained by subtracting filtered bathymetry from observed bathymetry. Fig. 2a shows the changes in mean amplitudes calculated by the median (blue line and circles) and DiM (red line and squares) filters. The DiM filter maximized the mean amplitude at 100 km filter width whereas the median filter maximized it at a filter width of 200 km. The regional bathymetry obtained from the DiM filter was smoothed by utilizing the median filter with 20 km filter width.

Fig. 2b shows that the DiM-based regional bathymetry closely approximated the rapid changes in depth due to the Kermadec Trench. The median-based regional, however, was not able to follow such changes (Fig. 2c). Fig. 2d and e compare the original bathymetry (black line) with the regional trends (blue line for median and red line for DiM) along the profiles shown in Fig. 1. The regional bathymetry using the median filter with 400 km filter width (purple line) is also shown for comparison because it was used for a previous flexure study at the LSC-03 (Contreras-Reyes et al., 2010). These regional trends along profile A-B (Fig. 2d) are relatively similar, except for a small-scale swell defined by the DiM filter (Fig. 2b). However, the DiM-based regional differs greatly from the median-based results along profile C-D (Fig. 2e). The applied median filters estimated the regional bathymetry to be too shallow at the trench; these biased results also affected the regional trends beneath the LSC-03.

Fig. 3 compares the residuals produced with the DiM (Fig. 3a) and median (Fig. 3b) filters. As discussed above (Fig. 2), the DiM-based residual bathymetry showed minimal effects from the trench, whereas the median-based residual still captures the depth variations of the trench. Based on the above analysis, we use the DiM-based regional and residual bathymetry for flexure modeling.

As the free-air gravity anomaly (FAA) is sensitive to both the flexure of the oceanic crust and the surface load (e.g., seamounts), it is widely utilized for various flexure studies (e.g., Adam and Bonneville, 2008; Altis, 1999; Kim and Wessel, 2010; Lyons et al., 2000; Paul and Singh, 1992; Zheng and Arkani-Hamed, 2002). In this study, however, the FAA reflects more signals from the trench than from the LSC-03 and its associated flexural moat (typically with negative FAA values around the seamount) (Fig. 4a). Thus, we estimated the residual gravity (Fig. 4c) by removing the regional trend (Fig. 4b) from the observed FAA (Fig. 4a). The DiM-based regional bathymetry was used with the variables listed in Table 1 to calculate the regional gravity. The observed gravity data are from the satellite-derived FAA grid version 23.1 (Sandwell and Smith, 2009). The residual gravity reduces the trench effects and enhances negative gravity anomalies resulting from flexure, which were not apparent in the observed gravity data. As the regional gravity data only considered the bathymetric curvature of the trench, the complex geology of the arc volcanism was not properly presented by the regional trend. It resulted in strong negative anomalies in the